Available online at www.sciencedirect.com

SCIENCE DIRECT®

Biochimica et Biophysica Acta 1606 (2003) 43–55

BIOCHIMICA ET BIOPHYSICA ACTA

BBA

www.bba-direct.com

Bidirectional electron transfer in photosystem I: electron transfer on the PsaA side is not essential for phototrophic growth in *Chlamydomonas*

Wendy V. Fairclough[a], Alec Forsyth[b], Michael C.W. Evans[b], Stephen E.J. Rigby[a], Saul Purton[b], Peter Heathcote[a,*]

[a] *School of Biological Sciences, Queen Mary, University of London, Mile End Road, London E1 4NS, UK*
[b] *Department of Biology, University College London, University of London, Gower Street, London WC1E 6BT, UK*

Received 11 February 2003; received in revised form 2 July 2003; accepted 4 July 2003

Abstract

We have used pulsed electron paramagnetic resonance (EPR) measurements of the electron spin polarised (ESP) signals arising from the geminate radical pair $P700^{\bullet+}/A_1^{\bullet-}$ to detect electron transfer on both the PsaA and PsaB branches of redox cofactors in the photosystem I (PSI) reaction centre of *Chlamydomonas reinhardtii*. We have also used electron nuclear double resonance (ENDOR) spectroscopy to monitor the electronic structure of the bound phyllosemiquinones on both the PsaA and PsaB polypeptides. Both these spectroscopic assays have been used to analyse the effects of site-directed mutations to the axial ligands of the primary chlorophyll electron acceptor(s) A_0 and the conserved tryptophan in the PsaB phylloquinone (A_1) binding pocket. Substitution of histidine for the axial ligand methionine on the PsaA branch (PsaA-M684H) blocks electron transfer to the PsaA-branch phylloquinone, and blocks photoaccumulation of the PsaA-branch phyllosemiquinone. However, this does not prevent photoautotrophic growth, indicating that electron transfer via the PsaB branch must take place and is alone sufficient to support growth. The corresponding substitution on the PsaB branch (PsaB-M664H) blocks kinetic electron transfer to the PsaB phylloquinone at 100 K, but does not block the photoaccumulation of the phyllosemiquinone. This transformant is unable to grow photoautotrophically although PsaA-branch electron transfer to and from the phyllosemiquinone is functional, indicating that the B branch of electron transfer may be essential for photoautotrophic growth. Mutation of the conserved tryptophan PsaB-W673 to leucine affects the electronic structure of the PsaB phyllosemiquinone, and also prevents photoautotrophic growth.

Keywords: Site-directed mutagenesis; Methionine; Tryptophan; PsaA and PsaB; PSI; A_0; A_1; ESP; ENDOR

1. Introduction

The photosystem I (PSI) reaction centre is a plastocyanin–ferredoxin oxidoreductase (see Ref. [1] for recent reviews). Light energy initiates electron transfer from the primary electron donor P700, which is a dimer of chlorophyll *a* molecules. The primary electron acceptor A_0 is a chlorophyll a monomer, which transfers electrons to a phylloquinone (vitamin K_1) secondary electron acceptor A_1. Subsequently, electrons are transferred to a bound [4Fe–4S] centre, F_X, and then on to two further bound [4Fe–4S] centres called F_A and F_B. The PSI reaction centre contains two major core proteins PsaA and PsaB [2], which show extensive sequence homology and form a heterodimeric complex binding P700, A_0, A_1, and F_X. During the last 10 years, two groups in Berlin have worked to resolve the X-ray crystal structure of the PSI complex from *Synechococcus elongatus*, and Fromme and Krauss with coworkers have recently published a new structure of a trimeric form of this complex at 2.5 Å resolution [3].

The publication of this structure enables the first detailed examination of structure–function relationships in this Type I reaction centre, which differs in many respects from the

Abbreviations: E_M, oxidation–reduction mid-point potential; ENDOR, electron nuclear double resonance; EPR, electron paramagnetic resonance; ESEEM, electron spin echo envelope modulation; ESP, electron spin polarised; OD, optical density; PAR, photosynthetically active radiation; PCR, polymerase chain reaction; PMS, phenazine methosulphate; PSI, photosystem I; P700, primary electron donor of photosystem I; $\Delta Hptp$, line width peak-to-peak of first derivative EPR spectrum; A_0, chlorophyll primary electron acceptor in photosystem I; A_1, phylloquinone secondary electron acceptor in photosystem I; F_A, F_B and F_X, [4Fe–4S] centres of photosystem I; PhQ, phylloquinone; hfc's, hyperfine couplings

* Corresponding author. Tel.: +44-207-882-3019; fax: +44-208-983-5489.

E-mail address: P.Heathcote@qmul.ac.uk (P. Heathcote).

0005-2728/$ - see front matter © 2003 Elsevier B.V. All rights reserved.
doi:10.1016/S0005-2728(03)00083-5

relatively well-characterized Type II photosynthetic reaction centres of purple photosynthetic bacteria [4]. Two of these differences have been addressed by the experiments presented in this study: the properties of the binding pocket for the primary electron acceptor A_0, and the route(s) of electron transfer in the PSI reaction centre.

Type I reaction centres function over a more reducing range of redox potentials than Type II, as they need to generate electrons with a sufficiently low redox potential to reduce $NADP^+$ to NADPH. The binding pockets of the primary and secondary electron acceptors show a number of unique features that may well explain the function of these components at relatively low redox potentials. The axial ligand to each of the chlorophylls that are candidates for the A_0 electron acceptor is provided by the sulphur of a methionine side chain. This provides a relatively weak ligand and could also serve to exclude water, which could potentially form a stronger ligand. The lack of a strong fifth ligand to the central magnesium of this chlorophyll, together with the hydrogen bonding of a tyrosine to the keto oxygen of ring V, have been identified [3,5] as particular elements of the A_0 binding pocket in PSI that may account for the relatively low redox potential at which the A_0 acceptor operates. Whereas the E_M of chlorophyll *a* reduction is ~ -900 mV in vitro [6], the E_M of $A_0/A_0^{\bullet -}$ is estimated at -1050 mV [7].

Another possible difference between Type II and Type I reaction centres is suggested by evidence indicating that electron transfer may take place along both branches of the PSI reaction centre. The structure of the PSI reaction centre [3,5] has apparent (pseudo) C_2 symmetry, with two possible routes of electron transfer from P700 to F_X via two alternative accessory chlorophylls, two alternative A_0 chlorophyll primary electron acceptors and two alternative A_1 secondary phylloquinone electron acceptors. These form two separate possible electron transfer chains, with the pairs of primary and secondary electron acceptors bound to either the PsaA or PsaB polypeptides. Experiments using either optical or electron paramagnetic resonance (EPR) spectroscopic measurements of $A_1^{\bullet -}$ reoxidation, together with biochemical or genetic modification of the PSI iron–sulphur centres, established an electron transfer path from A_1 to F_X with an electron transfer rate at room temperature of $t_{1/e} \approx 200$ ns [8–10]. We have used [11] site-directed mutagenesis of the conserved tryptophan PsaA-W693 of *Chlamydomonas reinhardtii* to show that this rate is associated with the phylloquinone bound to PsaA. Substitution of histidine or leucine for the tryptophan slows down forward electron transfer from A_1 to F_X by a factor of 2–3.

However, there have been reports in the literature that a faster rate of electron transfer from A_1 to F_X of ≈ 20 ns at room temperature could also be detected [12,13], although this varied between different PSI preparations. Joliot and Joliot [14] measured optical transients that they attributed to phyllosemiquinone oxidation, in whole cells of the green alga *Chlorella sorokiniana*. They observed two rates of oxidation, $t_{1/2} = 13$ and 140 ns at room temperature. The two phases are of approximately equal intensity. They suggested that electron transfer is in fact bidirectional and occurring on the PsaB branch as well as the PsaA branch, with initial electron transfer being randomly directed to either side of the reaction centre with the overall rate limited on each side by the A_1 to F_X rate [14]. This suggestion was supported by analysis of the site directed mutants of *C. reinhardtii*, PsaA-W693F and PsaB-W673F [15]. The fast phase of 13 ns seen in *C. reinhardtii* is slowed by the PsaB side mutation to 70 ns, and the 140 ns rate by the PsaA mutation to 490 ns. However, the extent to which electron transfer occurs on the PsaB branch of the PSI reaction centre is still a controversial topic, mainly because it has not proved possible to measure an EPR transient corresponding to the fast phase of phyllosemiquinone oxidation reported by Joliot and co-workers [14,15].

We have in the last year developed biochemical and paramagnetic resonance spectroscopic procedures that allow us to monitor electron transfer on the PsaB-branch redox cofactors, and which provide evidence for electron transfer on this branch, albeit in frozen samples. An electron spin polarised (ESP) transient EPR signal is known to arise from the geminate radical pair $P700^{\bullet +}/A_1^{\bullet -}$ in PSI [16–18]. In a recent experiment we have measured the decay of this ESP signal at 100 K [19]. At this temperature the rates recorded are thought to reflect the influence of two different protein environments (PsaA and PsaB) on the decay of the correlation of the $P700^{\bullet +}/A_1^{\bullet -}$ geminate radical pair, rather than actual recombination between $P700^{\bullet +}$ and $A_1^{\bullet -}$, since the rates obtained are an order of magnitude faster than the reported rate for electrons to return to $P700^{\bullet +}$ from $A_1^{\bullet -}$ [20]. One decay rate that can be observed in frozen PSI can be attributed to PsaA side electron transfer. However, two rates of decay can be observed if the F_X electron acceptor is pre-reduced, and we interpret the results as indicating that electron transfer from P700 can occur to either the A-side or B-side phylloquinone at 100 K [19].

Normally, illumination of PSI in the presence of dithionite at pH 8 and 205 K reduces one phyllosemiquinone per $P700^{\bullet +}$, and photoaccumulation at pH 8 and 220 or 230 K reduces one phyllosemiquinone and one chlorophyll anion (attributed to $A_0^{\bullet -}$) [21,22]. Proton electron nuclear double resonance (ENDOR) spectra from wild type (WT) and the PsaA-W693 mutants demonstrate that the phyllosemiquinone photoaccumulated under these conditions is that attributed to the PsaA branch of electron transfer [11,23]. However, photoaccumulation of *C. reinhardtii* PSI at pH 10 and 220 K produces a maximum of four spins per $P700^{\bullet +}$, and proton ENDOR spectra indicate that a second phyllosemiquinone is being photoaccumulated. This phyllosemiquinone has markedly different proton hyperfine couplings (hfc's) and is unaffected by mutation to PsaA-W693, confirming that it does not arise from the PsaA branch of electron transfer [24]. We therefore conclude that this is the PsaB phyllosemiquinone and that electron transfer from

P700 to A_1 can take place on the PsaB branch during photoaccumulation at 220 K.

We now report on the characterisation of three new site-directed mutants of *C. reinhardtii* in which the methionine axial ligand to the A_0 primary electron acceptors on the A and B sides (PsaA-M684 and PsaB-M664, respectively) have been changed to histidine, and the tryptophan PsaB-W673 has been changed to a leucine. We find that the PsaA-M684H mutation completely blocks electron transfer to the phylloquinone on the PsaA branch, although electron transfer to the PsaB phylloquinone is unaffected. This mutant is able to grow photoautotrophically, demonstrating that not only is electron transfer possible on the PsaB branch as well as the PsaA branch, but that electron transfer on the PsaB branch alone is sufficient to support growth. The corresponding PsaB-M664H mutation completely blocks kinetically competent electron transfer on the PsaB branch, although photoaccumulation of the PsaB phyllosemiquinone is still possible. This mutant is unable to grow photoautotrophically, suggesting that PsaA-branch electron transfer alone is not sufficient to support growth. The substitution of leucine for the conserved tryptophan PsaB-W673 affects the electronic structure of the phyllosemiquinone attributed to the PsaB branch [24], but not that of the phyllosemiquinone on the PsaA branch, confirming the assignment of this photoaccumulated phyllosemiquinone to PsaB. As with the PsaB-M664H mutation, the PsaB-W673L change blocks kinetically competent electron transfer to the PsaB phyllosemiquinone and prevents photoautotrophic growth.

2. Materials and methods

2.1. Creation of site-directed mutants

Site-directed changes were introduced into the PsaA and PsaB subunits by biolistic transformation of the wild-type *C. reinhardtii* strain CC-1021 essentially as described previously [11]. For the PsaA-M684H mutation, plasmid pBev1-Avr, which contains the *psaA-3* gene linked to the spectinomycin-resistance marker *aadA* [11], was engineered such that the methionine codon (ATG) at position 684 was changed to histidine (CAC). The mutation results in the loss of an *Mse*I site, allowing the discrimination between wild-type and the mutant *psaA-3* allele in transformants. For the *PsaB* mutations, plasmid pAF16 was used. This plasmid was made as follows: the 6.0-kb *Eco*RI chloroplast fragment (Eco14) containing *psaB* was cloned into a derivative of pBluescript in which the polylinker region has been replaced with *Nhe*I and *Eco*RI sites, creating pAF60. A unique *Bgl*II site was then engineered into pAF60 within the *psaB-trnG* intergenic region, 224 bp downstream of the *psaB* stop codon. The *aadA* marker was then introduced into the *Bgl*II site in the same orientation as *psaB* to create pAF16. Site-directed changes were introduced into *psaB* using a two-step polymerase chain reaction (PCR) strategy and the resulting PCR product cloned into pAF16 using the unique *Spe*I and *Nco*I sites that flank the modified region. For the PsaBM664H mutation, the methionine codon (ATG) at position 664 (see note below) was changed to histidine (CAC), resulting in the loss of an *Hsp*92II site. For the PsaBW673L mutation, the tryptophan codon (TTG) at position 673 was changed to leucine (CTG) and a silent change introduced in codon Q674 to create a *Pst*I site. All plasmid constructs were verified by DNA sequencing. The three plasmids were introduced into the *C. reinhardtii* chloroplast using the biolistic process and *aadA* transformants selected in dim light (<1 μE m^{-2} s^{-1}) on TAP plates containing spectinomycin [11]. Transformant colonies carrying the site-directed change were identified by molecular analysis of PCR products derived from *psaA-3* or *psaB*. These transformant lines were repeatedly re-streaked to single colonies under selective conditions to obtain homoplasmic lines in which all copies of the gene within the chloroplast carried the site-directed change.

Note: Our re-sequencing of *C. reinhardtii psaB* (Genbank acc. no. U57326) has resulted in the correction of a number of errors in the original sequence (acc. no. X05848); the most significant of which corrects the protein sequence immediately downstream of residue 200 from PELQR. to PESR. This results in the renumbering of residue M664 to M663 and W673 to W672. However, in order to maintain consistency with previous work (e.g. Ref. [15]), we have used the old numbering system in this paper.

2.2. Growth analysis

Strains were initially cultured in liquid TAP medium at 25 °C in darkness. The growth phenotype was then determined by spotting 5 μl of log-phase culture on: (a) acetate-containing medium (TAP medium) and incubating the plates either in the dim light [<1 μE m^{-2} s^{-1} photosynthetically active radiation (PAR)], moderate light (45 μE m^{-2} s^{-1}) or high light (240 μE m^{-2} s^{-1}); (b) minimal medium (HSM medium) and incubating in moderate or high light under aerobic or anaerobic conditions [11].

The photoautotrophic growth rate of PsaA-M684H was monitored in liquid HSM medium in comparison to WT *C. reinhardtii*. Cultures were grown to mid-log phase ($3-5\times10^6$ cells/ml) and then inoculated into fresh HSM medium, to a final $OD_{750\ nm}\cong0.1$. The diluted cultures were incubated at 25 °C with both continuous shaking at 120 rpm and illumination at 45 μE m^{-2} s^{-1}. Aliquots were removed at various time intervals, and the $OD_{750\ nm}$ measured.

2.3. Western blot analysis

Western blot analysis of whole cell extracts was carried out as described previously [11] using antibodies to PsaA and PsaD. The PsaA antibodies were obtained from K. Redding (University of Alabama). The PsaD antibodies were raised in rabbit using a mixture of two synthetic peptides

(YPEKVNAGRVGANQ and IKVKFSGRMMSPAEI) that correspond to regions of the mature *C. reinhardtii* PsaD.

2.4. Biochemical and spectroscopic analysis

Cells were harvested from large scale (16 l) cultures using a Millipore Pelicon filter system. The chloroplast membrane fraction was prepared by the procedure described by Diner and Wollman [25]. The membranes were washed to remove excess sucrose and suspended in 20 mM Tris–HCl pH 8.0 containing 100 mM NaCl. An enriched PSI preparation was made by treatment with digitonin following the procedure of Boardman [26] except that 1% digitonin was used. CW and kinetic EPR measurements were made on whole cells, thylakoid membrane preparations and digitonin PSI preparations at concentrations of 2–6 mg chlorophyll/ml. For kinetic measurements, samples in standard 3-mm quartz EPR tubes were reduced either with sodium ascorbate (10 mM) or sodium ascorbate (10 mM) and phenazine methosulphate (PMS, 100 μM) for 30 min in the dark prior to freezing in the dark in liquid nitrogen, or reduced with 11.5 mM sodium dithionite and photoaccumulated as described next. Samples were stored in liquid nitrogen in the dark. In order to photoaccumulate $A_1^{\bullet -}$ and $A_0^{\bullet -}$ the samples in standard EPR tubes were reduced for 30 min in the dark with sodium dithionite prior to freezing in liquid nitrogen. $A_1^{\bullet -}$ and $A_0^{\bullet -}$ radicals were then photoaccumulated by illumination at 205 or 220 K as described previously for pH 8 [21,27] and pH 10 [22,24]. Briefly this involves illumination of EPR samples in an unsilvered dewar with quartz halogen lamps at a photon flux density of 1500 μE m^{-2} s^{-1}.

2.5. Paramagnetic resonance spectroscopy (CW EPR, pulsed EPR and ENDOR)

CW EPR spectra were recorded on a JEOL RE1X or a Bruker ESP 300 spectrometer fitted with an Oxford Instruments ESR9 liquid helium cryostat. Kinetic pulsed EPR spectra and kinetics were measured as described previously [8] using a Bruker ESP380 X-band spectrometer with a variable Q dielectric resonator (Bruker Model 1052 DLQ-H 8907) fitted with an Oxford Instruments CF935 cryostat cooled with liquid nitrogen. Actinic illumination was supplied by an Nd-YAG laser (Spectra Physics DCR-11) with 10-ns pulse duration. ENDOR spectra were obtained at X-band using a Bruker ESP300 spectrometer as described by Rigby et al. [28,29].

3. Results

3.1. Effect of mutations on accumulation of photosystem I and growth phenotype

Previous work by ourselves and others (e.g. Refs. [30,31]) has shown that changes to key residues within PSI of *C. reinhardtii* can have a profound effect on the assembly or stability of the complex, resulting in a lack of accumulation of PSI within the cell. We therefore determined the level of PSI by Western blot analysis of whole-cell extracts using antibodies to the subunits PsaA and PsaD. The lower panel of Fig. 1 shows the level of PsaA and PsaD in each mutant. The changes to the methionine

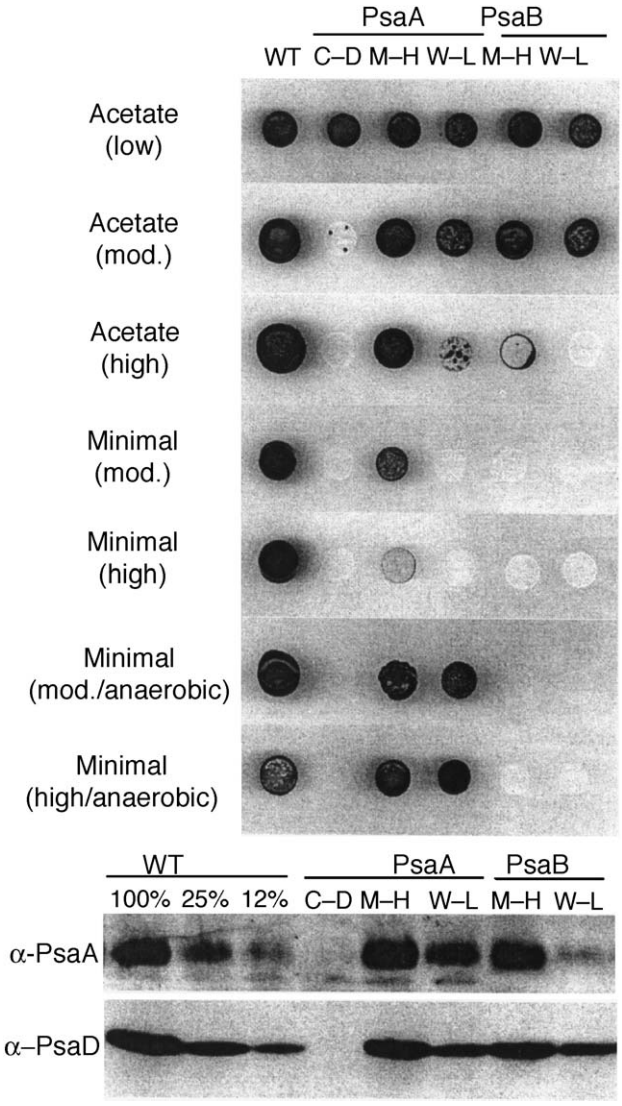

Fig. 1. Growth properties and accumulation of PSI in the mutants. Cultures of the wild-type (WT) strain and the three mutants, together with PsaA-W693L [11] and the PSI-deficient mutant PsaA-C575D [30], were grow in acetate medium in darkness and then spotted onto solid media. Medium containing acetate allows heterotrophic growth whereas minimal medium will support only photoautotrophic growth. Colonies were allowed to develop under different light levels: low (<1 μE m^{-2} s^{-1}); mod. (45 μE m^{-2} s^{-1}) or high (240 μE m^{-2} s^{-1}), and in the presence or absence of oxygen, as indicated. The lower panel shows immunoblots using antibodies to PsaA or PsaD. Equal loadings of whole cell extracts were separated on a 15% polyacrylamide gel and probed with the antibodies. To allow quantification, WT extract was diluted with the PsaA-C575D (C–D) extract to give 25% and 12% WT loadings.

ligands (PsaA-M684H and PsaB-M664H) appear to have a relatively minor effect with PSI accumulating to near wild-type levels in both cases. The substitution of the tryptophan associated with the B-side phylloquinone (PsaB-W673L) has a more deleterious effect with PSI levels approximately 20% of wild-type as judged by the level PsaD, and less as judged by the level of PsaA (Fig. 1). This is in contrast to the corresponding mutation in the A-side phylloquinone binding pocket (PsaA-W693L) where PSI levels are approximately 50% of wild type [11].

The growth phenotype of the mutants was examined under a range of conditions (Fig. 1). All three mutants are capable of heterotrophic growth on solid medium containing acetate, and are less sensitive to light than the PSI-deficient strain PsaA-C575D. However, the B-side mutants do display a light sensitivity when grown under high illumination. This light-sensitive phenotype in PSI mutants has been shown previously to be dependent on the presence of oxygen, with some mutants capable of phototrophic growth only under anaerobic conditions [32]. This is the case with the A-side mutant, PsaA-W693L [11] and to a lesser extent the PsaA-M684H mutant which displays reduced phototrophic growth in the presence of oxygen but normal growth in its absence (Fig. 1). Interestingly, this mutant has a growth rate comparable with that of the wild-type strain when grown in liquid minimal medium under moderate light. As shown in Fig. 1, neither of the B-side mutants is capable of photoautotrophic growth under either aerobic or anaerobic conditions.

3.2. Spectroscopic characterisation of the PsaA-M684H mutant of C. reinhardtii: electron transfer from P700 to F_A/F_B and photoaccumulation of $A_1^{\bullet -}$ and $A_0^{\bullet -}$

Initially, the ability of mutants to transfer electrons from the electron donor P700 to the terminal electron acceptors F_A/F_B was monitored using CW EPR (data not shown). In WT *C. reinhardtii* this electron transfer can be initiated by illumination of the sample at 15 K in the cryostat, and is essentially irreversible over the time scale of measurement. Illumination of digitonin PSI preparations of the PsaA-M684H mutant, frozen in the dark in the presence of sodium ascorbate, produced EPR signals corresponding to $P700^{\bullet +}$ and $(F_A/F_B)^-$. This demonstrates that electron transfer under these conditions (electron transfer from P700 to the bound FeS centres F_A/F_B at cryogenic temperatures) is not affected by the PsaA-M684H substitution, and also indicates that functional PSI is assembling in this mutant.

Digitonin PSI preparations of the PsaA-M684H mutant were then reduced with sodium dithionite at either pH 8 or pH 10 in the dark and frozen, as described in Materials and methods. These samples were then illuminated at 205 or 220

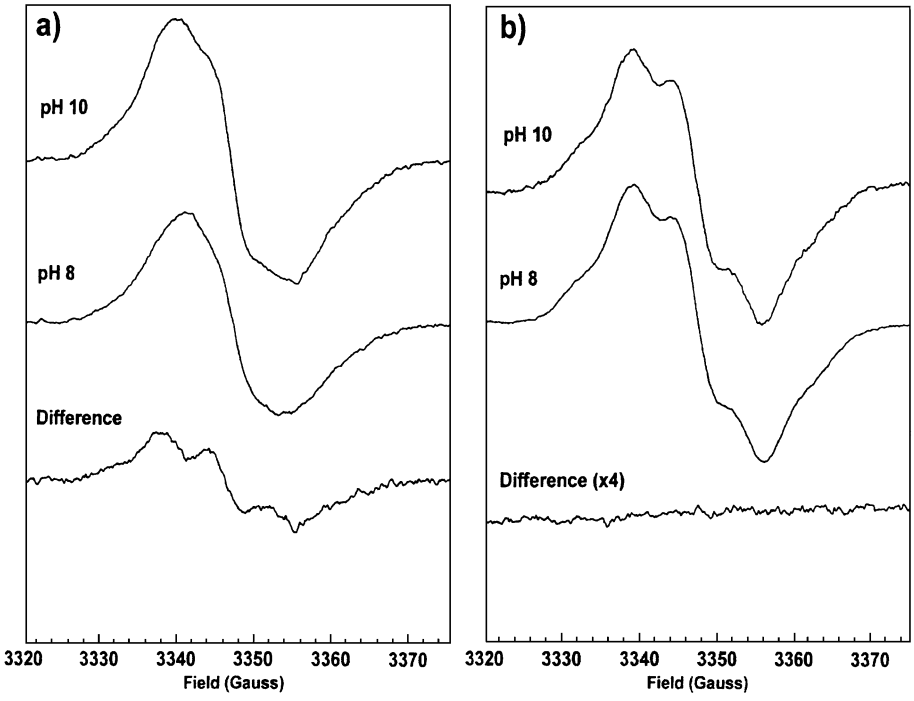

Fig. 2. EPR spectra of the g = 2.00 region of *C. reinhardtii* membranes following photoaccumulation in the presence of sodium dithionite at 220 K: (a) wild-type, (b) the PsaA-M684H mutant. The sample pH is given on the figure. pH 8 samples were photoaccumulated for 180 min, and pH 10 samples for 30 min. Difference spectra created by subtracting the spectrum of the pH 8 sample from that obtained at pH 10 are also shown. Experimental conditions: microwave power 40 μW; modulation amplitude 1.2 G; modulation frequency 12.5 kHz; temperature 70 K; each spectrum is the sum of four scans; measured using the ENDOR cavity.

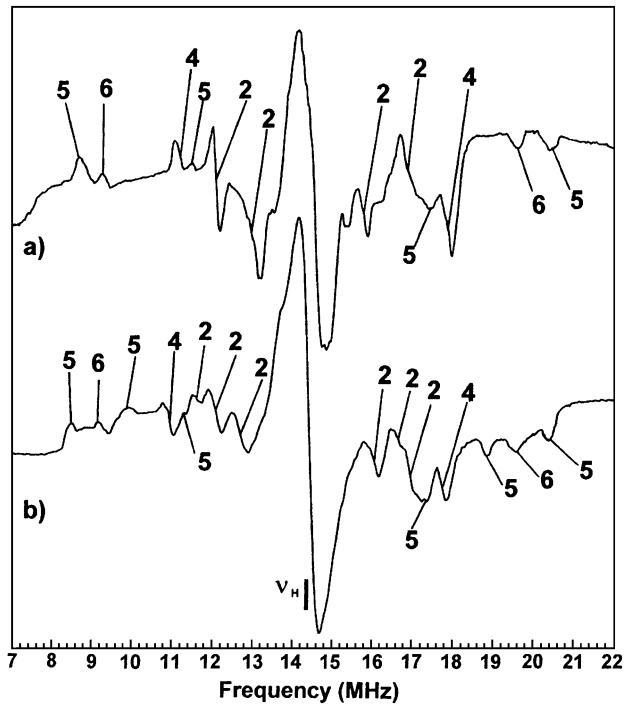

Fig. 3. ENDOR spectra of semiquinone radicals photoaccumulated in the presence of sodium dithionite in *C. reinhardtii* membranes: (a) the PsaA-M684H mutant photoaccumulated at pH 10 at 205 K for 5 min; (b) the PsaB-W673L mutant photoaccumulated at 220 K showing the spectrum produced by subtraction of a pH 8 sample from that obtained at pH 10 Times of photoaccumulation at different pH are as given in legend to Fig. 2. Experimental conditions: microwave power 7.9 mW; r.f. power 100 W; r.f. modulation depth 177 MHz; temperature 75 K; each spectrum is the sum of 200 scans.

K to monitor the photoaccumulation of the reduced primary and secondary electron acceptors in PSI.

Photoaccumulation of pH 8 samples at 205 K for 5 min in wild-type *C. reinhardtii* generates one spin per P700, assigned to PsaA:$A_1^{\bullet -}$ [11,21,22]. Photoaccumulation of PsaA-M684H under these conditions generated an EPR spectrum characteristic of the phyllosemiquinone radical, $A_1^{\bullet -}$, having an asymmetric line shape with a line width of approximately 8.75 gauss ($\Delta Hptp$). The spectrum also contained a minor contribution from a chlorophyll anion radical ($\Delta Hptp \cong 17.5$ gauss), which is observed as a

Table 1
Proton hyperfine couplings for PsaA phyllosemiquinone and PsaB phyllosemiquinone in WT, PsaA-M684H and PsaB-W673L

Feature	Proton hyperfine couplings (hfc's) in MHz[a]				Assignment
	PsaA PhQ	PsaB PhQ produced by subtraction	PsaB PhQ in PsaA-M684H	PsaB PhQ produced by subtraction in PsaB-W673L	
2	(−)4.5	(−)3.6	(−)3.0	(−)3.5	H-bond $A_\perp$
2	(−)6.2	(−)5.0	(−)5.0	(−)4.5	H-bond $A_\perp$
2				(−)5.0	H-bond $A_\perp$
5	N.D.	N.D.	6.0	6.0	H-bond $A_\parallel$
4	8.9	7.1	7.1	6.8	Methyl $A_\perp$
5				9.1	H-bond $A_\parallel$
6	12.0	10.5	10.5	10.3	Methyl $A_\parallel$
5	12.6	11.6	11.6	11.6	H-bond $A_\parallel$

[a] From ref. [34].

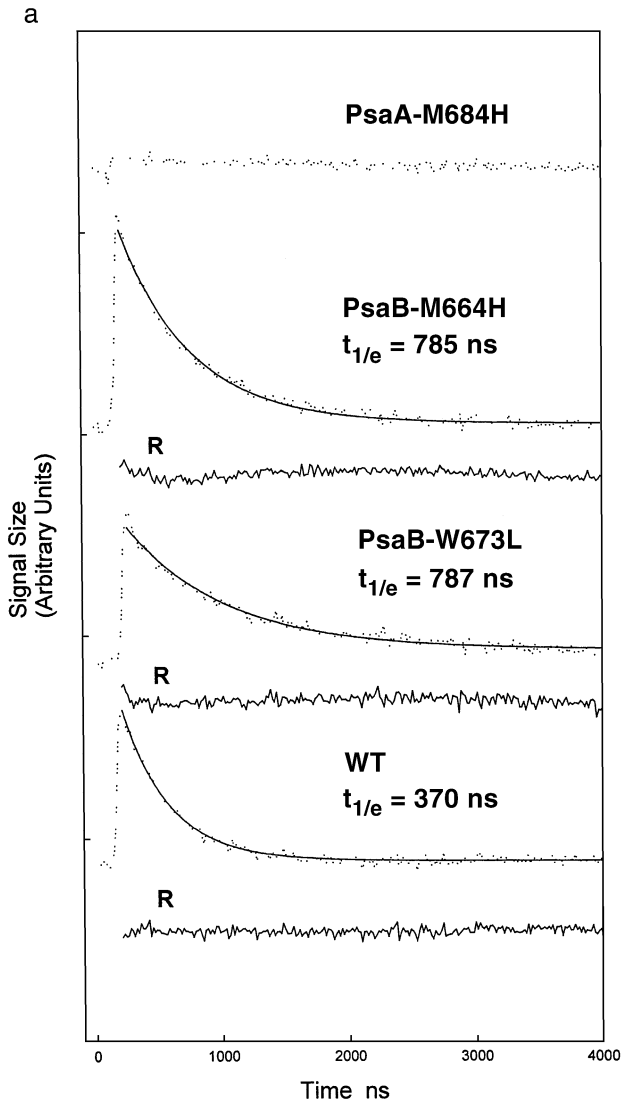

Fig. 4. Decay of the "out of phase" spin polarised signal at 265 and 100 K in WT and mutant strains of *C. reinhardtii*. Please note that traces shown are the results of single experiments, so the time constants for the fits shown differ from the averaged data results from a number of data sets presented in Table 2. The differences in the time constants arise between samples, rather than between separate measurements on the same sample. R is the residual from the fit. (a) Pulsed EPR kinetics were measured at 265 K as described in the Materials and methods. Samples reduced with ascorbate (20 mM) and phenazine methosulphate (200 μM) were illuminated by a 10-ns pulse from a doubled Nd:YAG laser with a flash repetition rate of 1 Hz. Signal intensity was measured at the peak of the out of phase signal near $g = 2.00$. Single exponential fits are shown as solid lines. (b) Pulsed EPR kinetics was measured at 100 K as described in the Materials and methods. Samples were reduced with sodium ascorbate (20 mM) or sodium dithionite (11.5 mM). Spectra were recorded from the dark-adapted samples, the dithionite samples were then illuminated at 205 K for 5 min and the kinetics measured again. Samples were illuminated by a 10-ns pulse from a doubled Nd:YAG laser with a flash repetition rate of 10 Hz. Signal intensity was measured at the peak of the out of phase signal near $g = 2.00$. Single or bi-exponential fits are shown as solid lines.

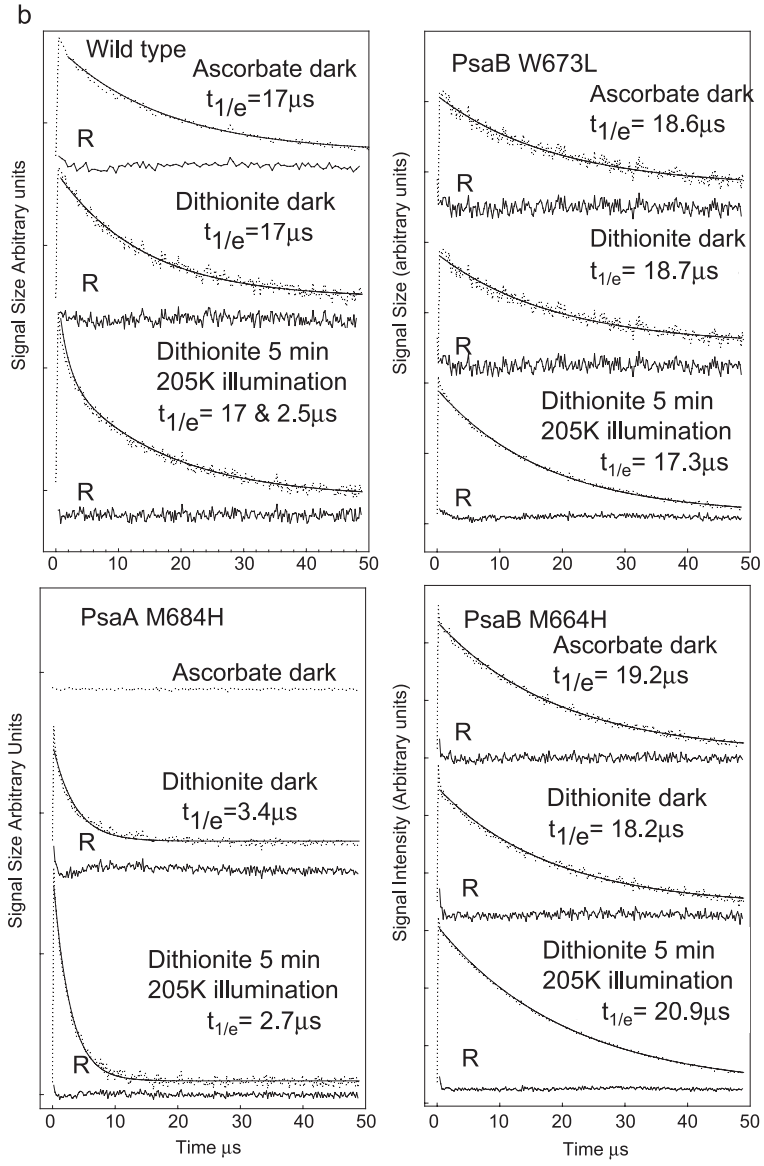

Fig. 4 (*continued*).

broadening of the high-field end of the spectrum in particular.

Photoaccumulation of pH 10 samples at 205 K for 2 min in wild-type *C. reinhardtii* generates one spin per P700, assigned to PsaA:$A_1^{\bullet -}$ [11,21,22]. This procedure was carried out for the PsaA-M684H mutant, and the resulting spectrum was again characteristic of the phyllosemiquinone radical, $A_1^{\bullet -}$ and contained minor contributions from a chlorophyll anion radical.

Photoaccumulation at 220 K and pH 8 or 10 of digitonin PSI preparations from PsaA-M684H reduced with sodium dithionite produced both a phyllosemiquinone radical and a chlorophyll anion radical (see Fig. 2b). However, subtraction of the pH 8/220 K spectrum from the pH 10/220 K spectrum produced a flat baseline (Fig. 2b), indicating that additional species were not photoaccumulated at pH 10/220 K compared to photoaccumulation at pH 8/220 K. This is in contrast to the results obtained with PSI from WT *C. reinhardtii* [24] (Fig. 2a) where the PsaB phyllosemiquinone and an additional chlorophyll anion species would be reduced at pH 10 and 220 K. So it seems that although photoaccumulation of the PsaA-M684H PSI at 205K and either pH 8 or 10 will reduce a phyllosemiquinone species (which in WT would be assigned to PsaA:$A_1^{\bullet -}$ [11,21,22]), photoaccumulation at pH 10 and 220 K does not reduce an additional phyllosemiquinone species as seen in WT [24]. This could suggest that either the PsaA or PsaB-branch phyllosemiquinone was not being photoaccumulated in PsaA-M684H, and since this is a mutant of the axial ligand to A_0 on the PsaA branch, it would seem likely that the PsaA-branch phyllosemiquinone is that affected. However, this cannot

be confirmed until the detailed electronic structure of the phyllosemiquinone that is photoaccumulated in PsaA-M684H is examined by proton ENDOR spectroscopy, which is capable of distinguishing between the PsaA and PsaB-branch phyllosemiquinones [24].

3.3. Spectroscopic characterisation of the PsaA-M684H mutant: proton ENDOR spectra of photoaccumulated phyllosemiquinone radical(s) $A_1^{\bullet -}$

Since it seems that the PsaA-M684H substitution has prevented photoaccumulation of one of the two phyllosemiquinones that could be photoaccumulated in PSI from WT *C. reinhardtii*, i.e. of either the PsaA or PsaB phyllosemiquinone, we decided to look in more detail at the proton ENDOR spectrum of the digitonin PSI preparation of PsaA-M684H photoaccumulated at pH 10 and 205 K. These are conditions that normally lead to photoaccumulation of one spin per P700 [21,22] attributed to the PsaA-bound phyllosemiquinone alone [11]. Examination of the CW-EPR spectrum of this photoaccumulated radical had previously suggested (see above) that this procedure had generated phyllosemiquinone (8.75 gauss) and a small amount of a species assigned to a chlorophyll anion radical (17.5 gauss). Using temperature and microwave conditions to minimise the contributions from the chlorophyll anion radical, a proton ENDOR spectrum was obtained (Fig. 3a and Table 1) which was indeed of a phyllosemiquinone, but was of the phyllosemiquinone attributed to the PsaB branch of electron transfer [24]. The spectrum contained none of the features attributed to the PsaA-bound phyllosemiquinone [33], and since it was obtained without the need to subtract one ENDOR spectrum from another as was previously required in WT samples photoaccumulated at pH 10 and 220 K which contained both the PsaA and PsaB-bound phyllosemiquinones [24], this represents a more accurate determination of the hfc's associated with the PsaB-bound phyllosemiquinone. The hfc's presented in Table 1 demonstrate that, in fact, the subtraction technique employed previously [24] had only affected one of the H-bond hfc's, that with the smallest hfc. Samples of PsaA-M684H photoaccumulated at pH 8 and 205 K for 90 min, which in WT samples would lead to the photoaccumulation of one spin per P700 [21,24] attributed to the PsaA phyllosemiquinone [11], yielded CW EPR spectra of a phyllosemiquinone (as described above) whose proton ENDOR spectrum was also that recently assigned to the PsaB phyllosemiquinone [24].

These results clearly demonstrate that photoaccumulation of the PsaA-bound phyllosemiquinone is prevented in PsaA-M684H.

3.4. Spectroscopic characterisation of the PsaA-M684H mutant: pulsed EPR measurements of forward electron transfer from $A_1^{\bullet -}$ to F_X, and of the decay of correlation of the ESP signal arising from the geminate radical pair $P700^{\bullet +}/A_1^{\bullet -}$

Thylakoid membrane samples of wild-type *C. reinhardtii* and PsaA-M684H were prepared with sodium ascorbate and PMS in order to study the decay of the ESP signal attributed to the $P700^{\bullet +}$/PsaA:$A_1^{\bullet -}$ radical pair [11] at 265 K. This decay reflects forward electron transfer from $A_1^{\bullet -}$ to F_X [8–10] on the PsaA branch of electron transfer [11] and in WT *C. reinhardtii* the $t_{1/e}$ is 355 ± 136 ns at 265 K [23] (see also Fig. 4a and Table 2). At 265 K no ESP signal could be detected in the PsaA-M684H mutant (Fig. 4a) suggesting that the $P700^{\bullet +}$/PsaA:$A_1^{\bullet -}$ radical pair is not being formed.

At 100 K the rates recorded for the disappearance of the ESP signal reflect the influence of two different protein environments (PsaA and PsaB) on the decay of the correlation of the $P700^{\bullet +}/A_1^{\bullet -}$ geminate radical pair [19]. An essentially monophasic decay rate of ≅17 μs can be observed in frozen PSI which can be attributed to PsaA-branch electron transfer. A biphasic decay can be observed if the F_X electron acceptor is pre-reduced by photoaccumulation of sodium dithionite-reduced samples at 205 K (Fig. 4b and Table 2), with a faster decay rate of $t_{1/e}$≅3 μs appearing in these circumstances which is attributed to PsaB-branch electron transfer [19].

Fig. 4b and Table 2 present the 100 K kinetic measurements for the PsaA-M684H mutant, in comparison to *C. reinhardtii* wild type. No "slow" phase of decay of correlation reflecting the PsaA-branch environment signal

Table 2
ESP decays ($t_{1/e}$) in thylakoid membrane preparations from WT and mutant strains of *C. reinhardtii*

Temperature of measurement	Treatment of sample	WT	PsaA-M684H	PsaB-M664H	PsaB-W673L
265 K	Ascorbate/dark	355(± 136) ns, n=20	No signal	749(± 96) ns, n=17[a]	889(± 160) ns, n=6
100 K	Ascorbate/dark	17 μs	No signal	17.7 (± 1.3) μs, n=12	18.7(± 0.7) μs, n=4
100 K	Dithionite/dark	17 μs	2.6(± 0.1) μs, n=8	19.8(± 1.6) μs n=16	16.9(± 0.4) μs, n=8
100 K	Dithionite/5 minutes illumination at 205 K	17.7(± 2.4) and 2.3(± 1) μs, ~ 70:30	2.3(± 0.1) μs, n=8	19.52(± 1.76) μs, n=12	17.7(± 0.48) μs, n=9
100 K	Dithionite/15 minutes illumination at 205 K	17.7(± 2.4) and 2.3(± 1) μs, ~ 55:45	N.D.	20.0(± 0.8) μs, n=14	17.4(± 1.14) μs, n=6

[a] 603(± 44) ns, n=8, in whole cells.

was observed in the PsaA-M684H mutant when frozen in the dark in the presence of sodium ascorbate or sodium dithionite, or after illumination at 205 K to reduce F_X. A monophasic rate is observed, of $t_{1/e}=2.3-2.6$ μs, with no contribution from the "slow" phase. These results are in agreement with those obtained from the photoaccumulation of radicals in PsaA-M684H (Fig. 3a and Table 1), indicating that electron transfer to the phylloquinone on the PsaA branch of electron transfer is blocked in this mutant.

3.5. Spectroscopic characterisation of the PsaB mutants, PsaB-M664H and PsaB-W673L: electron transfer from P700 to F_A/F_B, photoaccumulation of $A_1^{\bullet-}$ and $A_0^{\bullet-}$ and ENDOR spectra of $A_1^{\bullet-}$

The EPR signals corresponding to $P700^{\bullet+}$ and $(F_A/F_B)^-$ were observed when thylakoid preparations from PsaB-M664H and PsaB-W673L were illuminated at 15 K (data not shown), but the amount of $P700^{\bullet+}$ generated by illumination at cryogenic temperatures was noticeably reduced in these transformants compared to WT, suggesting that although irreversible electron transfer from $P700^{\bullet+}$ was possible under prolonged illumination at these cryogenic temperatures, the efficiency of this electron transfer was impaired. However, these results and those from the Western blot analysis confirm that functional PSI is assembling in these mutants. Samples of PsaB-M664H and PsaB-W673L were frozen at pH 8 and pH 10 in the presence of sodium dithionite and photoaccumulated at 220 K for 90 min (pH 8) or 30 min (pH 10), and the CW EPR spectra recorded. The samples photoaccumulated both a phyllosemiquinone and chlorophyll anion radical species (data not shown). Proton ENDOR spectra, acquired under conditions that minimised the chlorophyll anion radical contribution and maximised the phyllosemiquinone contribution, demonstrated that both the PsaA and PsaB side phyllosemiquinones were photoaccumulated (data not shown). This finding indicates that photoaccumulation of the PsaB-side phyllosemiquinone is not blocked in PsaB-M664H or PsaB-W673L. However, the proton ENDOR spectrum of the PsaB phyllosemiquinone [24] is altered by the PsaB-W673L substitution (Fig. 3 and Table 1) compared to WT, whereas the phyllosemiquinone photoaccumulated at pH 8 and 205 K attributed to the PsaA phyllosemiquinone [11,35] is unaffected by this substitution. These results demonstrate that the additional phyllosemiquinone species photoaccumulated in the presence of dithionite at pH 10 and 220 K is that bound to the PsaB polypeptide, as previously suggested [24]. The proton ENDOR spectrum of the PsaB phyllosemiquinone [24] is unaltered by the PsaB-M664H substitution, and at present we are unable to explain why this substitution on the PsaA branch should block photoaccumulation of the PsaA-branch phyllosemiquinone, and yet an identical substitution on the PsaB branch should not have this effect.

3.6. Spectroscopic characterisation of the PsaB mutants, PsaB-M664H and PsaB-W673L: pulsed EPR measurements of forward electron transfer from $A_1^{\bullet-}$ to F_X, and of the decay of correlation of the ESP signal arising from the geminate radical pair $P700^{\bullet+}/A_1^{\bullet-}$

Samples of PsaB-M664H were reduced with sodium ascorbate and PMS in order to study the decay of the ESP signal attributed to the $P700^{\bullet+}/A_1^{\bullet-}$ radical pair at 265 K. Fig. 4a and Table 2 present the 265 K pulsed EPR measurements for wild-type and the PsaB-M664H mutant. These data demonstrate that, although slowed by a factor of 2–3 compared to wild type, forward electron transfer on the PsaA-branch of PSI in PsaB-M664H is occurring. Although all the rates collected in Table 2 are from experiments on thylakoid membrane preparations, we also carried out experiments on whole cells of WT and mutant strains of *C. reinhardtii* in order to ensure that preparation of thylakoid membranes was not perturbing PSI function. In every case, the results were identical except for PsaB-M664H, where, as noted in Table 2, rates of forward electron transfer from A_1 to F_X as monitored by the ESP decay at 265 K were significantly slower in thylakoid membranes. In whole cells the M664H substitution in PsaB has only decreased the rate at 265 K by 50%.

We had previously reported that substitution of histidine or leucine for the conserved tryptophan PsaA-W693 of *C. reinhardtii* slows down forward electron transfer from A_1 to F_X on the PsaA branch (as measured by the decay of the ESP signal at 265 K) by a factor of 2–3 [11], or perhaps even blocks electron transfer. We had hoped that substitution of leucine for the equivalent tryptophan on PsaB (PsaB-W673L) would have a similar effect, and that, as a result, the rate of forward electron transfer from A_1 to F_X on the PsaB branch would become slow enough to be detected by the ESP technique. However, measurement of the decay of the geminate radical pair $P700^{\bullet+}/A_1^{\bullet-}$ at 265 K (Fig. 4a) in PsaB-W673L gave a decay that could be fitted as a single exponential decay with $t_{1/e}$ of ~900 ns. This could simply be explained as an effect of the PsaB-W673L substitution on forward electron transfer on the PsaA branch, although it could, in the absence of other evidence, be argued that there is an underlying contribution from the PsaB branch to the apparent rate of electron transfer that we are unable to resolve.

Sodium dithionite was used to reduce samples of PsaB-M664H and PsaB-W673L in order to measure 100 K ESP kinetics. Fig. 4b and Table 2 present the 100 K kinetic measurements for these mutants, in comparison to the wild-type strain. The rate of decay of the spin polarised signal attributed to the $P700^{\bullet+}/A_1^{\bullet-}$ radical pair in sodium ascorbate/PMS or sodium dithionite-reduced samples prior to photoaccumulation is monophasic for PsaB-M664H and PsaB-W673L and is comparable to wild type, indicating that the decay of the correlation of the $P700^{\bullet+}/A_1^{\bullet-}$ geminate radical pair [19] is that reflecting the PsaA-branch

environment [19]. Subsequent 205 K illumination of the sodium dithionite-reduced samples for 5 min to reduce F_X led to no change in the rate of decay. The biphasic rate observed for the WT is not seen in either PsaB-M664H or PsaB-W673L, indicating that there is no decay rate equivalent to that attributed to the PsaB environment in WT *C. reinhardtii* [19]. These data also indicate that although PsaA-branch electron transfer is functioning in PsaB-M664H and PsaB-W673L, electron transfer from P700 to the PsaB-branch phyllosemiquinone at 100 K is blocked.

4. Discussion

Since the initial evidence for two pathways of electron transfer in PSI relied upon the detection of two different rates of reoxidation of $A_1^{\bullet -}$ by optical spectroscopy [14], the debate has centred on whether this reflects electron transfer via the two possible branches of electron transfer utilising the PsaA- and PsaB-bound phylloquinones [14], or alternatively the A_1–F_X equilibrium model [36] (this topic is reviewed and discussed in the recent review by Brettel and Leibl [37]). In the A_1–F_X equilibrium model [36] it is proposed that the free energies of the states $P700^{\bullet +}A_1^{\bullet -}$ and $P700^{\bullet +}F_X^{\bullet -}$, connected to each other by a single pathway of electron transfer, are close to each other so that the forward and backward electron transfer rates between the two states are similar. In such a situation, establishment of a quasi-equilibrium between $P700^{\bullet +}A_1^{\bullet -}$ and $P700^{\bullet +}F_X^{\bullet -}$ gives rise to a fast phase of $A_1^{\bullet -}$ reoxidation, and depopulation of this quasi-equilibrium by electron transfer from $F_X^{\bullet -}$ to the next electron acceptor F_A gives rise to a slower phase of electron transfer. Brettel and Leibl [37] concluded that none of the arguments that could be presented against the two branch models was "waterproof", and added a note in proof that the results obtained by Guergova-Kuras et al. [15] studying the effects of PsaA-W693F and PsaB-W673F mutants of *C. reinhardtii* were most easily explained if one assumed that the faster phase of $A_1^{\bullet -}$ reoxidation reflects electron transfer from the PsaB phyllosemiquinone, and the slow phase reflected electron transfer forward from the PsaA phyllosemiquinone. However, this conclusion is still controversial, and it has been argued that mutations of a residue near the phylloquinone on one polypeptide could be having an indirect effect on electron transfer via the phylloquinone on the other polypeptide.

What is not disputed is the observation that forward electron transfer via the phyllosemiquinone is taking place on at least the PsaA polypeptide. There is general acceptance in the literature that the decay of the ESP signal attributed to the $P700^{\bullet +}/A_1^{\bullet -}$ radical pair occurring in around 200 ns at room temperature reflects forward electron transfer from $A_1^{\bullet -}$ to F_X [8,9], and that this corresponds to the slow phase of reoxidation of $A_1^{\bullet -}$ detected by optical spectroscopy [10,12,36]. We have shown [11] by site-directed mutagenesis of the conserved tryptophan PsaA-W693 of *C. reinhardtii* that this rate of ESP decay is associated with the phylloquinone bound to PsaA, and showed that photoaccumulation at pH 8 and 205/220 K or pH 10 and 205 K reduces the phyllosemiquinone bound to the PsaA polypeptide. These results were subsequently confirmed independently by mutagenesis of both PsaA-W693 and PsaB-W673 [35]. It has not proved possible so far to measure an ESP transient corresponding to the fast phase of reoxidation of $A_1^{\bullet -}$ detected by optical spectroscopy, but this could be due to insufficient time resolution of this technique.

The results obtained with the PsaA-M684H mutation demonstrate that electron transfer via the PsaA phyllosemiquinone is blocked by this substitution. Photoaccumulation at pH 10 and 220 K reduces the same two species (assigned to a phyllosemiquinone and a chlorophyll anion) as are photoaccumulated at pH 8 and 220 K (Fig. 2). This is in contrast to the results obtained in WT *C. reinhardtii* PSI, where photoaccumulation at pH 8 and 220 K reduces one phyllosemiquinone (that on the PsaA branch [11,34]) and one chlorophyll anion per P700. Photoaccumulation of WT at pH 10 and 220 K reduces a second phyllosemiquinone and chlorophyll anion per P700, with the additional phyllosemiquinone being attributed to the PsaB-bound $A_1^{\bullet -}$ [24]. In the PsaA-M684H samples neither of the species photoaccumulated has the proton hfc's formerly assigned to the PsaA phyllosemiquinone, demonstrating that this substitution has blocked electron transfer from P700 to A_1 on the PsaA polypeptide. The phyllosemiquinone photoaccumulated at pH 8 and 205 K or pH 10 and 205 K is not the PsaA phyllosemiquinone seen in WT [11], but a phyllosemiquinone with the hfc's assigned to the PsaB-bound $A_1^{\bullet -}$ (Fig. 3, Table 1) [24]. Since this ENDOR spectrum of the PsaB phyllosemiquinone is obtained without the need for subtraction of two separate ENDOR spectra, as was the case in our previous measurement of this spectrum [24], it represents a more accurate determination of the hfc's associated with the PsaB-bound $A_1^{\bullet -}$. In fact, all the previously reported hfc's (Table 1) are evident in this spectrum and identical to those previously reported with the exception of the hfc at 3.0 MHz attributed to a H-bond $A_\perp$ which was previously reported as 3.6 MHz [24]. In addition, we report here the measurement of an additional hfc to an H-bond $A_\parallel$ component, labelled feature 5, of 6.0 MHz.

Measurements of the effect of the PsaA-M684H substitution on the decay of the ESP signal measured at 265 and 100 K confirm that electron transfer from P700 to A_1 on the PsaA polypeptide is blocked. The decay of the ESP signal at 265 K in approximately 350 ns seen in WT *C. reinhardtii* PSI has been shown to monitor forward electron transfer from $A_1^{\bullet -}$ to F_X on the PsaA polypeptide [11]. This signal cannot be detected in PSI from PsaA-M684H (Fig. 4a and Table 2) demonstrating that electron transfer from P700 to A_1 on the PsaA polypeptide does not occur. No other decay at 265 K is detected, indicating that any ESP decay due to forward electron transfer from $A_1^{\bullet -}$ to F_X on the PsaB

polypeptide is too fast to detect with this technique. The "slow" phase of decay of the ESP signal at 100 K seen in WT samples reduced with sodium ascorbate and PMS or sodium dithionite has previously been attributed to decay of the correlation of the PsaA $P700^{\bullet+}/A_1^{\bullet-}$ radical pair, with the rate reflecting the environment of the radical pair on this polypeptide [19]. This "slow" decay is absent in the PsaA-M684H (Table 2 and Fig. 4b) mutation, with just a "fast" phase of decay detected. A significant "fast" phase of decay was only seen in WT *C. reinhardtii* PSI when F_X was reduced by photoaccumulation of the sodium dithionite-reduced sample. Here it is seen without photoaccumulation and remains unaltered in rate as the photoaccumulation is carried out. This confirms that charge separation between P700 and A_1 cannot occur on the PsaA polypeptide, but is continuing to occur on the PsaB polypeptide, in agreement with the results at 265 K and of the photoaccumulation experiments. The growth phenotype of the PsaA-M684H mutation (Fig. 1) demonstrates that not only is electron transfer occurring on the PsaB branch of electron transfer in the PSI of *C. reinhardtii*, but that PsaB-side electron transfer on its own in the absence of PsaA-side electron transfer is sufficient to support photosynthetic growth. These results cannot be explained by the "quasi-equilibrium" model [36], which assumes electron transfer on only one branch of PSI.

Both the substitutions on the PsaB branch of electron transfer also block kinetically competent electron transfer on the PsaB branch. In both PsaB-M664H and PsaB-W673L, the "fast" phase of decay at 100 K of the correlation of the ESP signal arising from the geminate radical pair $P700^{\bullet+}/A_1^{\bullet-}$, which is though to reflect the PsaB environment [19], is absent (Fig. 4b and Table 2). This indicates that electron transfer to the phyllosemiquinone on the PsaB branch is blocked. Both of these mutants also have an effect on the decay of the ESP signal at 265 K (Fig. 4a and Table 2) which monitors forward electron transfer from A_1 to F_X on the PsaA branch [11]. This suggests that these mutants are having "indirect" effects on PsaA-branch electron transfer, although the effect is relatively small for PsaB-M664H (50% increase in rate for whole cells) and more significant for PsaB-W673L, which is as might be predicted given the proximity of the PsaA and PsaB phylloquinone binding pockets [3].

Both PsaB-branch mutants are unable to grow photoautotrophically (Fig. 1). This might indicate that PsaB-branch electron transfer is not taking place, and that PsaA side electron transfer on its own is insufficient to support growth. It might be argued that since the PsaB-branch mutants have effects on PsaA-branch forward electron transfer, this conclusion should be qualified to indicate that PsaA-branch electron transfer on its own, when modified by the PsaB-branch mutations, is insufficient to support growth. However, the effect of the PsaB-M664H mutation on forward electron transfer on the PsaA branch is relatively small, particularly in whole cells (Table 2).

However, there is another possible objection to reaching this conclusion, that it is possible that the effect of the PsaB-branch mutants on phototrophic growth is a secondary effect, such as photoinhibition (the method used to make the growth conditions anaerobic does leave some oxygen present), or some other secondary mechanism. Until it has been established that these mutants do inhibit PSI activity, and until it has been shown that growth can be rescued by reversing the mutation, we can only conclude that phototrophic growth of *C. reinhardtii* under the conditions we have used is prevented in the PsaB-branch mutants, suggesting that the B branch of electron transfer may be essential for photoautotrophic growth.

The effects of the PsaB-M664H and PsaB-W673L substitutions on the PsaB branch are, however, different in one respect from the effect of the PsaA-M684H substitution on the PsaA branch. In the PsaB transformants, it is possible to photoaccumulate the PsaB-branch phyllosemiquinone (Fig. 3 and Table 1). So, although these substitutions inhibit kinetically competent electron transfer, they do not inhibit reduction of the phyllosemiquinone on the PsaB branch by the photoaccumulation technique. This is fortuitous since it allows us to monitor the effect of the PsaB-W673L substitution on the PsaB-branch phyllosemiquinone (Fig. 3b and Table 1), which allows us to confirm the assignment of this species to the PsaB phyllosemiquinone as previously suggested [24]. The effect of the PsaB-W673L substitution on the PsaB-branch phyllosemiquinone is almost identical to the effect of the PsaA-W693H substitution [11], but not the PsaA-W693L substitution, indicating that identical substitutions in the two different phylloquinone binding pockets do not necessarily have identical effects on the bound phyllosemiquinones.

It is not possible from measuring the ESP decays at 100 K to estimate the relative amounts of electron transfer on the PsaA and PsaB branches following a single turnover flash. However, the optical measurements of Joliot and collaborators [14,15] indicate that although the precise ratio varies from species to species, approximately equal amounts go up the two branches in *C. reinhardtii*. How this can be achieved in a system where the constituents of P700 (a chlorophyll *a* and chlorophyll *a* enol), and the environment provided to these pigments by the PsaA and PsaB polypeptides, exhibit a pronounced structural asymmetry [3] has yet to be established. What does seem to be the case from the results presented here is that modulation of electron transfer on one branch redistributes electrons to the other branch of electron transfer. This can be deduced from two observations:

(a) Normally, the PsaB phyllosemiquinone can only be photoaccumulated at pH 10 and 220 K in the presence of sodium dithionite [24], but in PsaA-M684H, when electron transfer is blocked on the PsaA branch, then the PsaB phyllosemiquinone can be photoaccumulated under conditions where only the PsaA phyllosemiqui

none would be photoaccumulated in WT (i.e. pH 8 and 205K or pH 10 and 205 K, Fig. 3a and Table 1).

(b) In WT it is necessary to photoaccumulate samples at 205 K in the presence of sodium dithionite to reduce F_X in order to see the "fast" phase of decay of correlation of the ESP signal at 100 K attributed to the PsaB polypeptide environment. However, in PsaA-M684H such a signal is seen in the sodium dithionite dark samples (Fig. 4b and Table 2).

Further experiments are now in progress to characterise the distribution of electron transfer in these mutants, by measuring the optical transients attributed to reoxidation of the phyllosemiquinones at room temperature [14,15].

Whilst this manuscript was being revised, three more papers were published directly addressing the issue of bidirectional electron transfer in the photosystem I reaction centre. Agalarov and Brettel [38] investigated the temperature dependence of the biphasic electron transfer (ET) from the secondary acceptor A_1 to F_X by flash absorption spectroscopy in PSI isolated from *Synechocystis* sp. PCC 6803. They concluded that whereas the slow phase of reoxidation was temperature-dependent, the fast phase was temperature-independent, and suggested that energetic parameters (most likely the driving forces) rather than the electronic couplings are different for electron transfer from the A-branch phyllosemiquinone to F_X compared to the B-branch phyllosemiquinone to F_X. Two alternative schemes of ET in PS I were presented and discussed, one of which envisaged bidirectional electron transfer and the other in which electron transfer was on one branch to the B-branch phyllosemiquinone, and then electron transfer to the A-branch phyllosemiquinone occurred via F_X. However, the observations presented in this manuscript, and previous reports that an ESP signal associated with electron transfer to the PsaA-bound phylloquinone can be detected [11,35] argue against the latter conclusion, since electron transfer to the A-branch phyllosemiquinone via F_X would prevent any ESP signal from the geminate radical pair $P700^{\bullet+}/A_1^{\bullet-}$ on the A branch. Although this leads to the conclusion that bidirectional electron transfer does occur in PSI from cyanobacteria, two other recent publications [39,40] argue that electron transfer in PSI from cyanobacteria occurs predominantly on the A branch.

Acknowledgements

We gratefully acknowledge the expert technical assistance from Laura W Wood, Susan Jones, Pathma Ratnesar and Antonio Casal. We thank Dr. Kevin Redding (University of Alabama) for the kind gift of antibodies, and Dr. Stefano Santabarbara for helpful discussions.

This work was supported by grants from the UK Biotechnology and Biological Sciences Research Council (BBSRC) (CO0350, 7809 and B18658), a BBSRC studentship to WVF, and a European Union TMR programme (contract no. FMRX-CT98-0214).

References

[1] BBA Special Issue, Type I photosynthetic reaction centres, In: P. Heathcote (Ed.), Biochim. Biophys. Acta, Bioenerg. 1507 (2001).
[2] L.E. Fish, U. Kuck, L. Bogorad, Two partially homologous adjacent light-inducible maize chloroplast genes encoding polypeptides of the P700 *chlorophyll-a* protein complex of photosystem I, J. Biol. Chem. 260 (1985) 1413–1421.
[3] P. Jordan, P. Fromme, H.T. Witt, O. Klukas, W. Saenger, N. Krauss, Three-dimensional structure of cyanobacterial photosystem I at 2.5 angstrom resolution, Nature 411 (2001) 909–917.
[4] P. Heathcote, P.K. Fyfe, M.R. Jones, Reaction centres: the structure and evolution of biological solar power, Trends Biochem. Sci. 27 (2002) 79–87.
[5] P. Fromme, P. Jordan, N. Krauss, Structure of photosystem I, Biochim. Biophys. Acta, Bioenerg. 1507 (2001) 5–31.
[6] I. Fujita, M.S. Davis, J. Fajer, Anion radicals of pheophytin and *chlorophyll a*: their role in the primary charge separations of plant photosynthesis, J. Am. Chem. Soc. 100 (1978) 6280–6282.
[7] K. Brettel, Electron transfer and arrangement of the redox cofactors in photosystem I, Biochim. Biophys. Acta, Bioenerg. 1318 (1997) 322–373.
[8] P. Moenne-Loccoz, P. Heathcote, D.J. MacLachlan, M.C. Berry, I.H. Davis, M.C.W. Evans, Path of electron-transfer in photosystem I—direct evidence of forward electron-transfer from A_1 to Fe-S_X, Biochemistry 33 (1994) 10037–10042.
[9] A. Van der Est, C. Bock, J. Golbeck, K. Brettel, P. Setif, D. Stehlik, Electron-transfer from the acceptor A_1 to the iron–sulfur centers in photosystem I as studied by transient EPR spectroscopy, Biochemistry 33 (1994) 11789–11797.
[10] J. Luneberg, P. Fromme, P. Jekow, E. Schlodder, Spectroscopic characterization of PS-I core complexes from thermophilic *Synechococcus* sp-identical reoxidation kinetics of A_1^- before and after removal of the iron–sulfur-clusters F_A and F_B, FEBS Lett. 338 (1994) 197–202.
[11] S. Purton, D.R. Stevens, I.P. Muhiuddin, M.C.W. Evans, S. Carter, S.E.J. Rigby, P. Heathcote, Site-directed mutagenesis of PsaA residue W693 affects phylloquinone binding and function in the photosystem I reaction center of *Chlamydomonas reinhardtii*, Biochemistry 40 (2001) 2167–2175.
[12] P. Mathis, P. Setif, Kinetic-studies on the function of A_1 in the photosystem I reaction center, FEBS Lett. 237 (1988) 65–68.
[13] P. Setif, K. Brettel, Forward electron-transfer from phylloquinone-A_1 to iron–sulfur centers in spinach photosystem I, Biochemistry 32 (1993) 7846–7854.
[14] P. Joliot, A. Joliot, In vivo analysis of the electron transfer within photosystem I: are the two phylloquinones involved? Biochemistry 38 (1999) 11130–11136.
[15] M. Guergova-Kuras, B. Boudreaux, A. Joliot, P. Joliot, K. Redding, Evidence for two active branches for electron transfer in photosystem I, Proc. Natl. Acad. Sci. U. S. A. 98 (2001) 4437–4442.
[16] M.C. Thurnauer, P. Gast, Q-band (35 GHz) electron-paramagnetic-resonance results on the nature of A_1 and the electron-spin polarization in photosystem I particles, Photobiochem. Photobiophys. 9 (1985) 29–38.
[17] R.R. Rustandi, S.W. Snyder, L.L. Freezel, T.J. Michalski, J.R. Norris, M.C. Thurnauer, J. Biggins, Contribution of Vitamin-K1 to the electron-spin polarization in spinach photosystem I, Biochemistry 29 (1990) 8030–8032.
[18] S.W. Snyder, R.R. Rustandi, J. Biggins, J.R. Norris, M.C. Thurnauer, Direct assignment of Vitamin-K1 as the secondary acceptor-A_1 in photosystem-I, Proc. Natl. Acad. Sci. U. S. A. 88 (1991) 9895–9896.
[19] I.P. Muhiuddin, P. Heathcote, S. Carter, S. Purton, S.E.J. Rigby,

J.H. Golbeck, Evidence from time resolved studies of the $P700^{\bullet+}/A_1^{\bullet-}$ radical pair for photosynthetic electron transfer on both the PsaA and PsaB branches of the photosystem I reaction centre, FEBS Lett. 503 (2001) 56–60.

[20] E. Schlodder, M. Falkenberg, K. Gergeleit, K. Brettel, Temperature dependence of forward and reverse electron transfer from A_1^-, the reduced secondary electron acceptor in photosystem I, Biochemistry 37 (1998) 9466–9476.

[21] P. Heathcote, J.A. Hanley, M.C.W. Evans, Double-reduction of A_1 abolishes the EPR signal attributed to A_1—evidence for C2 symmetry in the photosystem I reaction-center, Biochim. Biophys. Acta 1144 (1993) 54–61.

[22] F. MacMillan, J.A. Hanley, L. van der Weerd, M. Knupling, S. Un, A.W. Rutherford, Orientation of the phylloquinone electron acceptor anion radical in photosystem I, Biochemistry 36 (1997) 9297–9303.

[23] M.C.W. Evans, S. Purton, V. Patel, D. Wright, P. Heathcote, S.E.J. Rigby, Modification of electron transfer from the quinone electron carrier, A_1, of photosystem 1 in a site directed mutant D576⇒L within the Fe-S_X binding site of PsaA and in second site suppressors of the mutation in *Chlamydomonas reinhardtii*, Photosynth. Res. 61 (1999) 33–42.

[24] S.E.J. Rigby, I.P. Muhiuddin, M.C.W. Evans, S. Purton, P. Heathcote, Photoaccumulation of the PsaB phyllosemiquinone in photosystem I of *Chlamydomonas reinhardtii*, Biochim. Biophys. Acta, Bioenerg. 1556 (2002) 13–20.

[25] B.A. Diner, F.A. Wollman, Isolation of highly active Photosystem II particles from a mutant of *Chlamydomonas reinhardtii*, Eur. J. Biochem. 110 (1980) 521–526.

[26] N.K. Boardman, Sub-chloroplast fragments: digitonin method, Methods Enzymol. 23 (1970) 268–276.

[27] P. Heathcote, P. Moenne-Loccoz, S.E.J. Rigby, M.C.W. Evans, Photoaccumulation in photosystem I does produce a phylloquinone ($A_1^{\bullet-}$) radical, Biochemistry 35 (1996) 6644–6650.

[28] S.E.J. Rigby, J.H.A. Nugent, P.J. O'Malley, The dark stable tyrosine radical of photosystem II studied in three species using ENDOR and EPR spectroscopies, Biochemistry 33 (1994) 1734–1742.

[29] S.E.J. Rigby, J.H.A. Nugent, P.J. O'Malley, ENDOR and special triple resonance studies of chlorophyll cation radicals in photosystem II, Biochemistry 33 (1994) 10043–10050.

[30] B.J. Hallahan, S. Purton, A. Ivison, D. Wright, M.C.W. Evans, Analysis of the proposed Fe-S_X binding region of Photosystem I by site directed mutation of PsaA in *Chlamydomonas reinhardtii*, Photosynth. Res. 46 (1995) 257–264.

[31] K. Redding, F. MacMillan, W. Leibl, K. Brettel, J. Hanley, A.W. Rutherford, J. Breton, J.-D. Rochaix, A systematic survey of conserved histidines in the core subunits of photosystem I by site-directed mutagenesis reveals the likely axial ligands of P700, EMBO J. 17 (1998) 50–60.

[32] J.-D. Rochaix, N. Fischer, M. Hippler, Chloroplast site-directed mutagenesis of photosystem I in *Chlamydomonas*: electron transfer reactions and light sensitivity, Biochimie 82 (2000) 635–645.

[33] S.E.J. Rigby, M.C.W. Evans, P. Heathcote, ENDOR and Special Triple resonance spectroscopy of $A_1^{\bullet-}$ of photosystem I, Biochemistry 35 (1996) 6651–6656.

[34] S.E.J. Rigby, M.C.W. Evans, P. Heathcote, Electron nuclear double resonance (ENDOR) spectroscopy of radicals in photosystem I and related Type 1 photosynthetic reaction centres, Biochim. Biophys. Acta, Bioenerg. 1507 (2001) 247–259.

[35] B. Boudreaux, F. MacMillan, C. Teutloff, R. Algarov, F.F. Gu, S. Grimaldi, R. Bittl, K. Brettel, K. Redding, Mutations in both sides of the photosystem I reaction center identify the phylloquinone observed by electron paramagnetic resonance spectroscopy, J. Biol. Chem. 276 (2001) 37299–37306.

[36] P. Setif, K. Brettel, Forward electron-transfer from phylloquinone-A_1 to iron–sulfur centers in spinach photosystem I, Biochemistry 32 (1993) 7846–7854.

[37] K. Brettel, W. Leibl, Electron transfer in photosystem I, Biochim. Biophys. Acta, Bioenerg. 1507 (2001) 100–114.

[38] R. Agalarov, K. Brettel, Temperature dependence of biphasic forward electron transfer from phylloquinone(s) A_1 in photosystem I: only the slower phase is activated, Biochim. Biophys. Acta, Bioenerg. 1604 (2003) 7–12.

[39] W. Xu, P. Chitnis, A. Valieva, A. van der Est, J. Pushkar, M. Krzystyniak, C. Teutloff, S.G. Zech, R. Bittl, D. Stehlik, B. Zybailov, G. Golbeck, J.H. Golbeck, Electron transfer in cyanobacterial photosystem I: I. Physiological and spectroscopic characterization of site-directed mutants in a putative electron transfer pathway from A_0 through A_1 to F_X, J. Biol. Chem. 278 (2003) 27864–27875.

[40] W. Xu, P. Chitnis, A. Valieva, A. van der Est, K. Brettel, M. Guergova-Kuras, J. Pushkar, S.G. Zech, D. Stehlik, G. Shen, B. Zybailov, J.H. Golbeck, Electron transfer in cyanobacterial photosystem I: II. Determination of forward electron transfer rates of site-directed mutants in a putative electron transfer pathway from A_0 through A_1 to F_X, J. Biol. Chem. 278 (2003) 27876–27887.